Contribution from General Electric Company,
Corporate Research and Development, Schenectady, New York 12301

Preparation and Monolayer Properties of Surfactant Tris(2,2′-bipyridine)ruthenium(II) Derivatives

S. J. VALENTY,* D. E. BEHNKEN, and G. L. GAINES, JR.*

Received March 16, 1979

The synthesis, characterization, and monolayer properties of three ruthenium bipyridyl complexes possessing hydrolytically stable surfactant linkages and differing molecular charges are described: $\{Ru^{II}(bpy)_2[bpy(C_{19}H_{39})_2]\}^{2+}$, **2**; $\{Ru^{II}(bpy)(CN)_2[bpy(C_{19}H_{39})_2]\}^0$, **3**; and $\{Ru^{II}[bpy(COO^-)_2]_2[bpy(C_{19}H_{39})_2]\}^{2-}$, **4**. Field-desorption mass spectra are reported for these and other nonvolatile ruthenium bipyridyl complexes. While the monolayer absorption spectra show no significant changes (except for iodide), both the surface pressure–area (Π–*A*) isotherms and luminescence spectra of **2** are strongly dependent on dissolved anions; perchlorate is observed to condense the films and provide higher emission intensity as compared to chloride. Such effects are unique to the interfacial environment and are not observed in homogeneous solutions of **2**. In contrast, the Π–*A* isotherm and luminescence of **3** are independent of anion. The Π–*A* isotherm of **4** does not show significant differences for subphases containing either Na^+ or Ca^{2+}. The emission intensity and maximum of **4** in 20% aqueous THF solution are pH dependent.

Irradiation of tris(2,2′-bipyridine)ruthenium(II) in a homogeneous solution of an appropriate electron donor or acceptor leads to a short-lived charge separation.[1] The possibility that the presence of a phase boundary might influence the kinetics of electron transfer such that the light-generated oxidizing and reducing potential could be physically separated and converted into stable, energy-storing products by further chemical reaction[2-6] has prompted the study of surfactant derivatives of tris(2,2′-bipyridine)ruthenium(II) constrained in monolayer films.[7-11] In the first such compound, **1**, prepared by Sprintschnik, Sprintschnik, Kirsch and Whitten,[7] the hydrocarbon tail was attached to the hydrophilic chromophore via an ester linkage which was shown to be easily hydrolyzed in monolayer films spread on neutral to slightly alkaline aqueous subphases.[8,12] Interestingly, the mechanical and luminescence properties of these positively charged monolayers were found to depend strongly on the anions contained in the subphase.[8] In order to eliminate the complications of hydrolysis and to extend our ability to control the nature of the monolayer film, we have synthesized, and report the characterization and monolayer properties of, ruthenium bipyridyl complexes **2**–**4** possessing hydrolytically stable surfactant linkages and differing molecular charges.

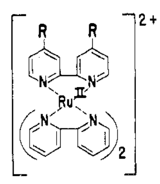

1, $R = -COOC_{18}H_{37}$
2, $R = -C_{19}H_{39}$
3, $R = -CH_3$

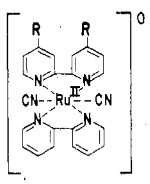

3, $R = -C_{19}H_{39}$
6, $R = -H$

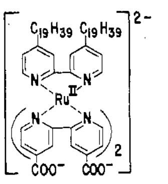

4

Experimental Section

Ruthenium trichloride hydrate (36.5% Ru, Alfa-Ventron), 2,2′-bipyridine (Aldrich or Fluka-SG), *n*-octadecyl chloride (97%, Lachat), 4-methylpyridine (Aldrich, distilled from KOH), Raney nickel (50/50 Ni–Al Alfa-Ventron), and analytical grade inorganic reagents were used. 4,4′-Dimethyl-2,2′-bipyridine (G. Frederick Smith) was oxidized to 2,2′-bipyridyl-4,4′-dicarboxylic acid and esterified to the diethyl ester by published methods.[8] *cis*-Dichlorobis(2,2′-bipyridine)ruthenium(II)[7] and *cis*-dicyanobis(2,2′-bipyridine)ruthenium(II), **6**,[13] were also synthesized according to literature procedures. Reactions were done under a nitrogen atmosphere (purified by passing N_2 through activated beds of Ridox and calcium sulfate).

Infrared spectra (Perkin-Elmer 457, KBr pellets), proton magnetic resonance spectra (Varian T-60, solution relative to Me_4Si), absorption spectra of monolayers (General Electric[8]), and field-desorption mass spectra (FDMS) (Varian-Mat 731) were obtained in a routine manner. Melting points were measured on a Fisher-Johns apparatus and are reported uncorrected. Elemental analyses were performed by Galbraith Laboratories (Knoxville, TN) and the Materials Characterization Branch of this laboratory.

High-pressure liquid chromatographic analyses of compounds **2**, **4**, and **5** were done by using established conditions.[14] Compound **2** could also be analyzed with a $MeOH/H_2O$ mobile phase containing methane sulfonate anion. Compounds **3** and **10** were eluted from a Chromegabond-NH_2 column (30 cm × 0.46 cm, 10-μm particles, ES Industries, Marlton, NJ) with a 15 min linear solvent gradient, 100% $CHCl_3$ to 15% MeOH in $CHCl_3$, at 2.0 mL/min and detected optically at 280 nm. The column equilibration time between analyses was ca. 7 min.

Formation, manipulation, and characterization of the monolayer films follows procedures previously published.[8] In a recent modification to the optical spectrometer used to record the absorption and emission spectra of glass-supported monolayer films, the base-line compensator has been replaced by a digital oscilloscope (Model 2090 III, Nicolet Instrument Corp.) which allows automatic blank correction and storage of spectra on magnetic disks.

4-Nonadecylpyridine (8). Into a 300-mL flask equipped with a mechanical stirrer, N_2 inlet, pressure-equalizing addition funnel, and thermostated oil bath, were added 14.8 g of sodium amide (0.38 mol) and 64.0 mL of 4-methylpyridine (61.1 g, 0.656 mol). The mixture was stirred under N_2 for 1 h while a color change to deep red was observed. A 110-mL sample of *n*-octadecyl chloride (95.0 g; 0.33 mol) was added to the rapidly stirred reaction mixture over a period of 1.5 h. Shortly after addition was begun, the reaction was warmed to 60 °C to prevent solidification and was subsequently stirred overnight at 100 °C. The reaction mixture was cooled to room temperature, diluted with 200 mL of chloroform, washed three times with 200 mL of H_2O, and reduced to dryness with the rotary evaporator. The resultant dark brown product was vacuum distilled three times at 0.07 mmHg to finally afford 48.8 g of constant-boiling (180 °C (0.07 mmHg)), white, waxy solid (0.141 mol, 43% yield based on *n*-octadecyl chloride). VPC analysis (6 ft × 2 mm ID OV-101, 285 °C, 25 psi He): one peak at 11.8 min.

Anal. Calcd for $C_{24}H_{43}N$: C, 83.4; H, 12.5; N, 4.1. Found: C, 83.6; H, 12.7; N, 4.0. IR (KBr): 3070, 3025, 2910, 2855, 1600, 1557, 1467, 1415, 1220, 996, 804, 725 cm^{-1}. UV ($CHCl_3$): 257 nm (ϵ 1.86 $\times 10^3$ M^{-1} cm^{-1}), 308 (1.7×10^2). ^1H NMR (60 MHz, $CDCl_3$): δ 0.87 (t, ~3 Hz), 1.23 (br s), 2.60 (t, 3 Hz), 7.10 (d, 3 Hz), 8.50 (d, 3 Hz).

4,4′-Dinonadecyl-2,2′-bipyridine (9). A 40.0-g sample of Ni–Al alloy was used to prepare the W7-J Raney nickel catalyst by the method of Badger and Sasse.[15] A 28.5-g sample of **8** (4.34×10^{-2} mol) in 80.0 mL of *o*-xylene (distilled from sodium) was added through an addition funnel into a 500-mL flask containing the active Raney nickel catalyst. The addition funnel was replaced with a condenser, and the reaction was refluxed 22 h under N_2. After the reaction mixture was cooled slightly, the catalyst was removed by vacuum filtration (**Caution**: pyrophoric!), the xylene filtrate was refrigerated, and a white precipitate was observed to form. The solid was collected

0020-1669/79/1318-2160$01.00/0

by vacuum filtration and recrystallized from absolute EtOH to yield 4.09 g of white powder (5.94 × 10^{-3} mol, 14.4% yield), mp 85.0–85.5 °C. An 18.25-g sample of **8** (5.28 × 10^{-2} mol) was recovered by vacuum distillation of the xylene filtrate (180 °C (0.07 mmHg)) for a total mass yield of 78.4%.

Anal. Calcd for $C_{48}H_{84}N_2$: C, 83.6; H, 12.3; N, 4.1. Found: C, 83.8; H, 12.3; N, 4.2. IR (KBr): 3060, 3020, 2920, 2850, 1598, 1547, 1470, 847, 723 cm^{-1}. UV (CHCl$_3$): 285 nm (ϵ 1.3 × 10^4 M^{-1} cm^{-1}). ^1H NMR (60 MHz, CDCl$_3$): δ 0.85 (t, 2.5 Hz) and 1.30 (br s) (74 H), 2.65 (t, 4 Hz, 4 H), 7.10 (dd, 3 Hz, 2H), 8.25 (s, 2 H), 8.50 (dd, 2.5 Hz, 2 H).

$\{Ru(bpy)_2[bpy(C_{19}H_{39})_2]\}(ClO_4)_2$ (2a). A 0.200-g sample of **9** (2.90 × 10^{-4} mol) and 25 mL of 95% ethanol were added to a 50-mL flask equipped with a reflux condenser, N_2 gas inlet, and magnetic stirrer. The solution was deoxygenated by reflux under N_2 for 1 h, and 0.156 g of $Ru(bpy)_2Cl_2\cdot3H_2O$ (2.90 × 10^{-4} mol) was added. The reaction was refluxed 3.0 h, under N_2 and cooled, and the product was precipitated by the slow addition of 25 mL of 0.10 M NaClO$_4$. Collection of the crude product and subsequent recrystallization from acetone afforded 0.282 g of red-orange solid (2.17 × 10^{-4} mol, 75% yield). High-pressure LC analysis: 3 mol % $\{(bpy)_2Ru^{II}[bpy(C_{17}H_{36})(C_{19}H_{39})]\}^{2+}$, ~1 mol % $\{(bpy)_2Ru^{II}[bpy(C_{19}H_{39})(C_{21}H_{43})]\}^{2+}$, ~3 mol % H_2O soluble Ru complexes.

Anal. Calcd for $C_{68}H_{100}N_6O_8Cl_2Ru$: C, 62.75; H, 7.74; Cl, 5.45; N, 6.46; Ru, 7.77. Found: C, 62.97; H, 7.86; Cl, 5.45; N, 6.42; Ru, 7.57. FDMS: mass ~1198 (M – ClO$_4$). IR (KBr): 3120, 3080, 2925, 2855, 1615, 1605, 1550, 1467, 1448, 1423, 1080, 767, 733, 723, 623 cm^{-1}. UV (CHCl$_3$): 258 nm (sh, ϵ 2.2 × 10^4), 290 (7.7 × 10^4), 400 (sh, 5.6 × 10^3), 433 (sh, 1.1 × 10^4), 459 (1.2 × 10^4).

$\{Ru(bpy)_2[bpy(C_{19}H_{39})_2]\}(Cl)_2$ (2b). The procedure is the same as that for **2a** except 0.10 M NaCl replaces NaClO$_4$. High-pressure LC analysis: as for **2a**. FDMS (^{102}Ru): mass 1102 (M – 2Cl). IR (KBr): 3015, 3005, 2910, 2840, 1610, 1600, 1463, 1440, 1420, 770, 730 cm^{-1}. UV–vis (CHCl$_3$): 254 nm (sh, ϵ 2.0 × 10^4), 291 (6.3 × 10^4), 357 (sh, 6.3 × 10^3), 400 (sh, 6.3 × 10^3), 435 (sh, 1.1 × 10^4), 457 (1.2 × 10^4).

$\{Ru(bpy)_2[bpy(CH_3)_2]\}(ClO_4)_2$ (5). A 0.180-g sample of 4,4′-dimethyl-2,2′-bipyridine (9.77 × 10^{-4} mol) and 150 mL of 95% ethanol were added to a 250-mL flask equipped with a reflux condenser, N_2 gas inlet, and magnetic stirrer. The solution was deoxygenated by reflux under N_2 for 1 h, and 0.500 g of $Ru(bpy)_2Cl_2\cdot3H_2O$ (9.77 × 10^{-4} mol) was added. The reaction was refluxed under N_2 for 3 h, and cooled, and the solvent was removed by rotary evaporation. The crude, dark red solid was dissolved in 100 mL of H_2O, the solution was filtered, and the product precipitated with the addition of 1.0 N HClO$_4$. The resultant red solid was collected and recrystallized from hot H_2O to yield 0.674 g of red crystals (8.46 × 10^{-4} mol, 87% yield).

Anal. Calcd for $C_{32}H_{28}Cl_2H_6O_8Ru$: C, 48.25; H, 3.54; Cl, 8.90; N, 10.55; Ru, 12.69. Found: C, 48.41; H, 3.68; Cl, 8.92; N, 10.43; Ru, 12.36. FDMS (^{102}Ru): mass 697 (M – ClO$_4$). IR (KBr): 3070, 1618, 1602, 1480, 1465, 1445, 1420, 1090 (vs), 765, 730, 625 cm^{-1}. UV–vis (H_2O): 247 nm (ϵ 2.1 × 10^4), 255 (sh, 1.9 × 10^4), 287 (6.5 × 10^4), 354 (sh, 4.0 × 10^3), 394 (sh, 4.8 × 10^3), 433 (sh, 1.0 × 10^4), 457 (1.1 × 10^4).

$Ru^{II}[bpy][bpy(C_{19}H_{39})_2][CN]_2$ (3) and $Ru^{II}[bpy(C_{19}H_{39})_2]_2[CN]_2$ (10). A 497.8-mg sample of **9** (7.22 × 10^{-4} mol), 112.8 mg of 2,2′-bipyridine (7.22 × 10^{-4} mol), and 700 mL of 2-propanol were added to a 1-L flask equipped with a reflux condenser, N_2 inlet, and magnetic stirrer. The solution was brought to reflux, 200 mg of $RuCl_3\cdot nH_2O$ (36.5% Ru, 7.22 × 10^{-4} mol) added, and the reaction refluxed 48 h. Most of the 2-propanol was distilled off (~100 mL remained), and the reaction was diluted with a degassed solution of 600 mL of methanol containing 700 mg of NaCN (1.43 × 10^{-2} mol). The reaction was refluxed an additional 16 h and then cooled, and solvent was removed by rotary evaporation. The collected red solid was dissolved in 100 mL of dichloromethane, washed three times with 50 mL of H_2O, and dried over Na_2SO_4, and the solution was filtered and reduced to dryness. The crude product was resolved into its respective components by chromatography on silica gel. Compound **10** was eluted with 5% methanol/toluene and **3** eluted with 10% methanol/toluene.

Compound **3** was recrystallized twice from 95% EtOH and dried under vacuum to yield 123 mg of orange powder (1.23 × 10^{-4} mol, 17% yield). High-pressure LC analysis: single component, 7.7 min. Anal. Calcd for $C_{60}H_{92}N_6Ru$: C, 72.17; H, 9.29; N, 8.42; Ru, 10.12. Found: C, 70.6; H, 9.3; N, 8.1; Ru, 11.8. FDMS (^{102}Ru): mass 998. UV–vis (CHCl$_3$): 285 nm (sh, ϵ 4.1 × 10^3), 295 (5.6 × 10^3), 345 (9.7 × 10^3), 370 (sh, 8.0 × 10^3), 450 (sh, 6.0 × 10^3), 502 (1.0 × 10^4). IR (KBr): 3062, 2920, 2850, 2070, 1615, 1465, 1442, 1420, 770, 730, 720 cm^{-1}.

High-pressure LC analysis of compound **10**: single component, 5.4 min. Anal. Calcd for $C_{98}H_{168}N_6Ru$: C, 76.9; H, 11.1; N, 5.5; Ru, 6.6. Found: C, 76.6; H, 11.2; N, 5.5; Ru, 7.9. FDMS (^{102}Ru): mass 1531. UV–vis (CHCl$_3$): 285 nm (sh, ϵ 4.1 × 10^4), 295 (5.6 × 10^4), 343 (1.0 × 10^4), 365 (sh, 8.6 × 10^3), 460 (sh, 6.8 × 10^3), 501 (1.0 × 10^4). IR (KBr): 3050, 2920, 2850, 2070 (doublet), 1612, 1465, 1420, 835, 720 cm^{-1}. The Π–A curve in comparison to that for **3** on distilled water is given in Figure 3 (supplementary material).

$Ru^{II}[bpy(COOC_2H_5)_2]_2[Cl]_2$ (7). Into a 250-mL flask equipped with a reflux condenser and N_2 inlet were added 2.40 g of diethyl 2,2′-bipyridyl-4,4′-dicarboxylate (7.99 × 10^{-3} mol), 1.11 g of $RuCl_3\cdot nH_2O$ (36.5% Ru, 4.00 × 10^{-3} mol), and 100 mL of *N,N*-dimethylformamide. The reaction was refluxed 4 h and most of the DMF removed by rotary evaporation. The collected solid was refluxed in 200 mL of 50% aqueous ethanol for 1 h, 50 g of LiCl was cautiously added, and the ethanol was removed by fractional distillation. The solution was cooled in an ice bath for 2 h, and the product was collected by vacuum filtration, washed with cold H_2O, and vacuum dried at 60 °C overnight. A 2.372-g sample of black microcrystalline product was collected (3.07 × 10^{-3} mol, 77% yield).

Anal. Calcd for $C_{32}H_{32}Cl_2N_4O_8Ru$: C, 49.75; H, 4.18; Cl, 9.18; N, 7.25; Ru, 13.08. Found: C, 49.62; H, 4.16; Cl, 9.34; N, 7.18; Ru, 12.95. IR (KBr): 3060, 3020, 2980, 2930, 1960, 1720, 1602, 1550, 1467, 1410, 1370, 1320, 1300, 1268, 1123, 1015, 770 cm^{-1}. UV–vis (CHCl$_3$): 312 nm (sh, ϵ 2.9 × 10^4), 322 (4.1 × 10^4), 433 (1.4 × 10^4), 589 (1.4 × 10^4).

$\{Ru^{II}[bpy(COOH)_2]_2[bpy(C_{19}H_{39})_2]\}(ClO_4)_2$ (4). A 223-mg sample of **9** (3.24 × 10^{-4} mol) and 250 mL of ethanol were brought to reflux under N_2, and 250 mg of **7** (3.24 × 10^{-4} mol) was added. The reaction was refluxed 3 days and cooled in an ice bath, and 47 mg of unreacted **9** was collected by vacuum filtration. The filtrate was diluted with 100 mL of dichloromethane, washed with 100 mL of aqueous 10^{-3} M HClO$_4$ and 10^{-2} M NaClO$_4$, dried over Na_2SO_4, filtered, and reduced to dryness to yield 404 mg of dark red solid. High-pressure LC analysis revealed the presence of an unidentified impurity which was largely removed by recrystallization from 60 mL of 10% H_2O in MeOH. The filtrate was reduced to dryness, and the collected solid was hydrolyzed 2 days in 500 mL of 20% H_2O/THF containing 10^{-3} M KOH. The reaction was diluted with 200 mL of CHCl$_3$ and washed three times with 200 mL of 10^{-2} M HClO$_4$. The organic layer was separated, dried, filtered, and reduced to dryness. The collected solid was recrystallized from 5% H_2O/acetonitrile (0.1 M HClO$_4$), giving 214 mg (1.45 × 10^{-4} mol, 45%) of a dark red solid. High-pressure LC analysis: single component, 7.0 min. Anal. Calcd for $C_{72}H_{100}N_6O_{16}Cl_2Ru$: C, 58.5; H, 6.8; N, 5.7. Found: C, 61.3; H, 7.2; N, 5.9. IR (KBr): 3420, 3080, 2920, 2850, 1723, 1615, 1550, 1470, 1410, 1375, 1310, 1235, 1095, 900, 770, 720, 623 cm^{-1}. UV–vis (20% aqueous THF): 259 nm (sh, ϵ 2.3 × 10^4), 284 (4.8 × 10^4), 293 (sh, 4.6 × 10^4), 404 (sh, 7.9 × 10^3), 446 (sh, 1.2 × 10^4), 478 (1.3 × 10^4).

Results and Discussion

Synthesis and Characterization of 2, 3, and 4. The synthesis of the surfactant ligand, 4,4′-di-*n*-nonadecylbipyridine (**9**), used a low-yield (14%) Raney nickel coupling reaction of 4-*n*-nonadecylpyridine (**8**) which had been prepared by alkylating the carbanion derived from 4-methylpyridine with *n*-octadecyl chloride in 43% yield. Attempts to prepare **9** by the dialkylation of 4,4′-dimethylbipyridine were not successful. In a fashion similar to the preparation of **1**,[7,8] the ruthenium surfactant complex, **2**, was obtained by reacting equimolar amounts of $Ru^{II}(bpy)_2(Cl)_2$ and **9**. Reverse-phase high-pressure LC with a *n*-octadecyl hydrocarbon-bonded stationary phase and a mobile aqueous organic (THF, MeOH) phase containing methanesulfonate anion has been used to provide an analytical measure of purity and a means of maintaining control over mass balance during various monolayer manipulations. Field-desorption mass spectra (FDMS) of **2a** (ClO_4^- salt) and **2b** (Cl^- salt) give molecular ions at masses of 1198 and 1102, respectively. Whereas the molecular ion of **2b** shows the loss of both anions, that of **2a** shows the loss

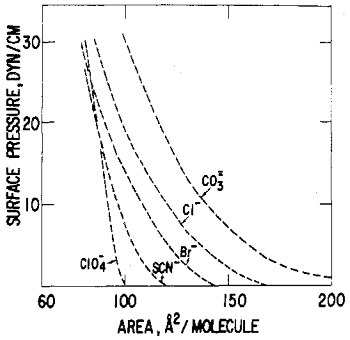

Figure 1. Surface pressure–molecular area isotherms of **2** on aqueous subphases 0.01 M in salt at 22–24 °C.

of only one. The FDMS of **5** (ClO_4 salt) also gives a molecular ion (^{102}Ru mass 697) in which a single perchlorate ion is retained.

The synthesis of **3** by reacting equimolar amounts of $Ru^{III}Cl_3$, 2,2′-bipyridine, and **9** followed by an addition of excess NaCN led to a mixture of ruthenium complexes. After extraction of the water-soluble compounds, the surfactant-containing portion of the mixture was separated by preparative column chromatography on silica gel. A 17% yield of monosurfactant ligand complex, **3**, was obtained in addition to the disurfactant ligand complex, **10**. After a survey of many different normal- and reverse-phase columns and solvent systems, it was found that these dicyanoruthenium complexes could be analyzed by high-pressure LC with an amino-modified stationary phase and a $CHCl_3$–MeOH gradient mobile phase. FDMS of the cyano compounds gave stronger molecular ions than those observed for **2** and **5**: specifically, masses (^{102}Ru) of 466, 998, and 1531 for **6**, **3**, and **10**, respectively.

The formation of **7** from the previously synthesized[8] 4,4′-bis(carboethoxy)-2,2′-bipyridine ligand (77% yield), its reaction with **9**, and its subsequent alkaline hydrolysis provide the synthetic route to **4** (45% yield). Compound **4** is very insoluble in all organic solvents in which the other surfactant complexes, **1**, **2**, and **3**, are solubilized. The need to add 10^{-2} M $HClO_4$ to acetonitrile in order to dissolve **4** suggests an oligomeric form in which the ionized carboxylate groups of one complex form salt linkages with two or more other complexes.

Surface Pressure–Area (Π–*A*) Isotherms. When monolayers of **2**, **3**, and **4** are spread on alkaline subphases, the area at constant surface pressure remains unchanged with time in contrast to the decrease in area observed[8,12] for films of **1** formed under identical circumstances. Films of **2** recovered from the air–alkaline subphase interface and analyzed by high-pressure LC show no difference from material not cast into monolayers.

As is the case for **1**, Π–*A* curves of **2** have a marked dependence on subphase counterion (Figure 1). All films are stable and reversible except for that formed on ClO_4^-. In the latter case, the initial compression is unstable with Π, decreasing slowly for $120 > A > 100$ Å², $\Pi <$ dyn/cm. After compression above 10 dyn/cm, the film gives the stable and reversible Π–*A* curve shown. While all of the counterions used give converging molecular areas at high Π for both **1** and **2**, e.g., 80–85 Å² on ClO_4^- at $\Pi = 30$ dyn/cm, the areas of **2** at 10 dyn/cm are 10–15% smaller than those of **1**. The surface potentials of **1** and **2** on 0.01 M NaCl are very similar: $\Delta V \approx 500$–600 mV. On 0.01 M $NaClO_4$, ΔV for **2** decays with time (probably due to slow stabilization of the film), reaching values <100 mV.

The Π–*A* isotherms of monolayers formed from the uncharged surfactant **3** show little difference whether ClO_4^- or Cl^- is the subphase counterion (Figure 2) or, indeed, whether any salt is present (Figure 3, supplementary material). Such behavior is consistent with that observed for other neutral monolayer films, such as those formed from the long-chain alcohols.[16]

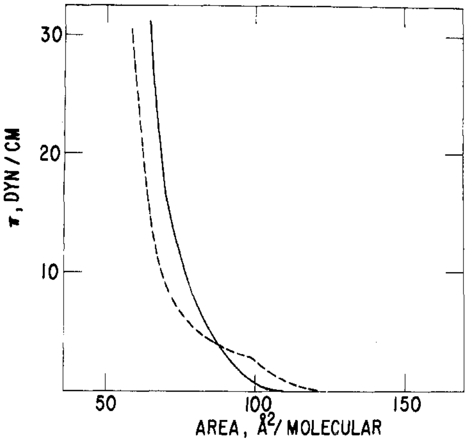

Figure 2. Surface pressure–molecular area isotherms of **3** on aqueous subphases 10^{-3} M in NaCl (- - -) and $NaClO_4$ (—) at 23 °C.

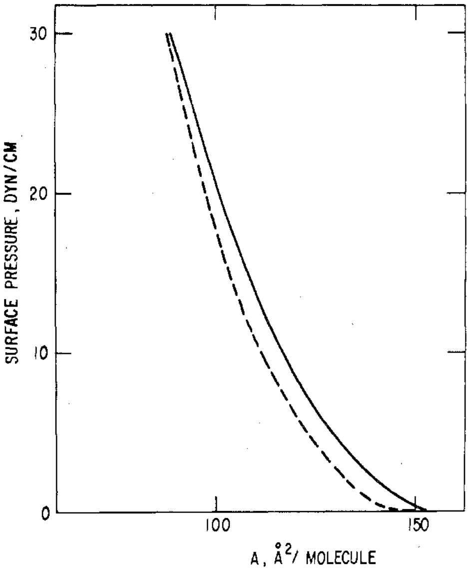

Figure 4. Surface pressure–molecular area isotherms of **4** on aqueous subphases 10^{-2} M in NaCl (—) and $CaCl_2$ (- - -) at 23 °C.

Calcium and other polyvalent cations radically alter the Π–*A* curves and mechanical properties of ionized fatty acid monolayers spread at the air–water interface.[17] In contrast, the Π–*A* curves of **4** on 0.01 M NaCl, $CaCl_2$, $NaClO_4$, and NaOH show only small differences (Figure 4). Such results suggest more intramolecular salt linkages between Ca^{2+} and two carboxylate groups bound to the same ruthenium complex than intermolecular linkages binding two different ruthenium complex molecules.

Absorption Spectroscopy. Monolayers of **2** can be transferred reproducibly from a variety of subphases onto hydrophilic quartz slides. Figure 5 provides a comparison of the absorption spectra of **2** as a quartz-supported monolayer (uncorrected for reflection occurring at the substrate–air interface) and as an equal number of molecules in $CHCl_3$. Within ±10% absorption, the visible spectra of monolayers of **2b** transferred from aqueous 0.01 M $NaClO_4$, NaBr, NaCl, and NaF are identical whereas for those transferred from 0.01 M NaI the discrete long-wavelength absorption (ca. 460 nm) has become a shoulder on a more strongly absorbing band extending into the ultraviolet (~370 nm is the lower wavelength limit of the monolayer spectrometer). Also shown are

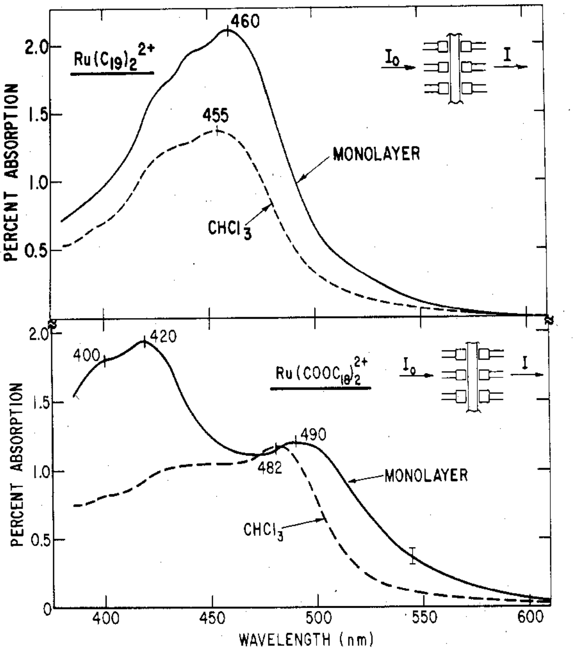

Figure 5. Absorption spectra of **1** (lower) and **2** (upper) as single monolayers on both sides of a hydrophilic quartz slide transferred from 10^{-3} M $NaClO_4$ (Π = 30 dyn/cm, 21 °C) and as an equilvalent number of molecules in $CHCl_3$ solution.

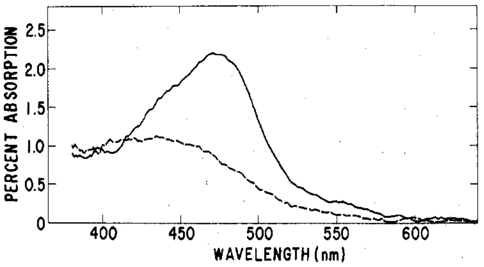

Figure 6. Absorption spectra of **3** (---) and **4** (—) as single monolayers on both sides of a hydrophilic quartz slide transferred from 10^{-3} M NaCl at 21 °C.

the corresponding spectra for **1**. While the band shapes of the monolayer and $CHCl_3$ solution spectra are much the same for **2**, such is not the case of **1**. By analogy to the absorption spectra of $\{Ru^{II}[bpy(COOCH_3)_2]_3\}^{2+}$, $\lambda_{max}(H_2O)$ 510 nm,[18] the long-wavelength absorption bands of **1** at 482 and 490 nm can tentatively be assigned to the MLCT transition[19-21] in which the excited-state charge density is localized on the ligand bearing the carboalkoxy substituents. The shorter visible wavelength (420, 430 nm) absorptions may then result from MLCT transitions to the unsubstituted ligands. Hence, the difference in spectra of **1** as a monolayer and in solution may well be due to the selective orientation of the ligands in the film as well as to solvent effects on the MLCT transition. The spectra of **2** show no such difference, perhaps because the alkyl-substituted ligand is electronically very similar to the unsubstituted 2,2′-bipyridine.

Monolayers of **3** and **4** can also be transferred routinely to hydrophilic quartz from 10^{-3} M aqueous $NaClO_4$. The featureless broad absorption band of **3** as a monolayer (Figure 6) has little similarity to its solution spectrum in $CHCl_3$ (tabulated in Experimental Section). As Demas et al.[22] have reported, the absorption and emission spectra of **6** are solvent dependent. In fact, the monolayer spectrum of **3** looks similar to that of **6** in H_2O (λ_{max} ~430 nm[22]). It should be noted that the monolayer spectra of **3** reported here were obtained on films which had been at the air–water interface for only ca. 5 min and within 10–15 min after being transferred to the quartz plate. The absorption spectra (in $CHCl_3$) of monolayers of **3** recovered from the surface of separate subphases containing 0.01 M NaCl and 0.01 M $NaClO_4$ after extended periods show significant, but presently not explained, changes. No changes in absorption spectra with time were observed for **6** in either aqueous $NaClO_4$ or NaCl solutions.

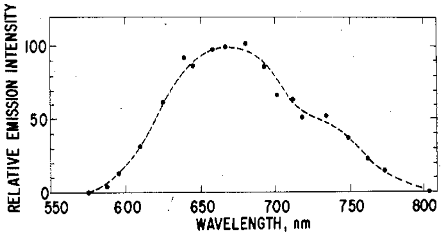

Figure 7. Luminescence spectrum of **2b** formed as a monolayer on 0.01 M NaCl at ca. 5 dyn/cm.

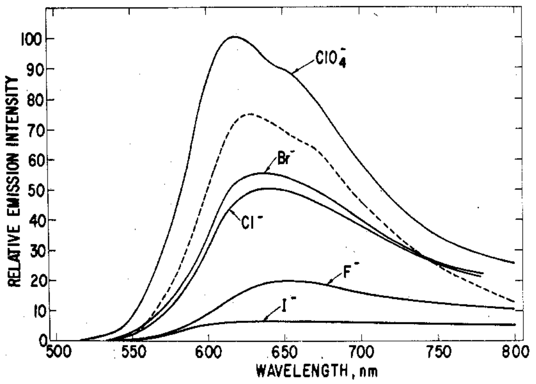

Figure 8. Corrected luminescence spectra of **2b** as single monolayers on both sides of a hydrophilic quartz slide transferred from freshly prepared aqueous subphases 10^{-3} M in NaX (Π = 30 dyn/cm; 21 °C) and in $CHCl_3$ solution (---).

The absorption spectrum of **4** as a monolayer (Figure 6) cannot be compared directly to its solution spectrum in $CHCl_3$ due to insolubility. However, the spectrum (in $CHCl_3$) of the closely related compound $\{Ru^{II}[bpy(C_{19}H_{39})_2][bpy(COOC_2H_5)]_2\}(ClO_4)_2$[23] provides a near-perfect match in both band-maxima positions and their relative optical densities.

Luminescence Spectroscopy. When excited at 436 nm, solutions of either **2a** or **2b** in both $CHCl_3$ and 20% aqueous THF and **5** in H_2O produce a red luminescence at the same wavelength maximum, 625–630 nm, and of the same relative intensity (±6%). Similarly, no solvent effect was observed in the absorption spectra of these solutions. In contrast, both the absorption and emission spectra of **1** are quite different in $CHCl_3$ and 20% aqueous THF.[8,14] For instance, when a change is made from $CHCl_3$ to 20% aqueous THF solutions of **1**, the emission maximum is red shifted from 685 to 718 nm, and the relative intensity decreases by 50%. The emission quantum yield of $\{Ru^{II}(bpy)_2[bpy(COOCH_3)_2]\}^{2+}$ in a totally aqueous solution is 25% of that for **1** in $CHCl_3$(Φ_L = 0.18).[18] No spectral dependence upon the nature of the counterion has been observed for any of these compounds in homogeneous solution.

The luminescence spectrum of **2** formed as a monolayer on aqueous 0.01 M NaCl is shown in Figure 7. The luminescence intensity does not vary with time. The total emission, λ >600 nm, for films of **2** on 0.01 M $NaClO_4$ is ca. sevenfold greater than on 0.01 M NaCl.

The corrected luminescence spectra of **2** in $CHCl_3$ solution and as monolayers supported on hydrophilic quartz after transfer from aqueous 10^{-2} M $NaClO_4$, NaBr, NaCl, NaF, and NaI (**2b** was spread) are compared in Figure 8. The exciting light at 436 nm (bandwidth 3.5 nm) was absorbed equally (±8%) by all the supported monolayers except that formed on I^- which had ca. 25% greater optical density even though the deposition ratio was 1.1. Both the position of the luminescence maximum and its intensity are affected by the counterion: λ_{max} order ClO_4^-, $I^- < Br^- < Cl^- < F^-$; relative intensity order $I^- < F^- < Cl^-$, $Br^- < ClO_4$. These observations parallel the behavior previously reported for **1**.[8] For both compounds, the difference in emission intensities between perchlorate and chloride was greater for films constrained at the air–aqueous salt interface than that for those films transferred to solid supports.

The emission intensity of quartz-supported monolayers of **3** does not depend on either the counterion (ClO_4^-, Cl^-) in the subphase from which the film was transferred or the counterion (ClO_4^-, Cl^-) in the aqueous solution in contact with the monolayer during the measurement. Whereas the corrected emission maxima of **3** in $CHCl_3$ and **6** in aqueous solution are 670 and 630 nm, respectively, with intensity falling off toward the red, the luminescence of the quartz-supported film of **3** has a shoulder at ca. 660–670 nm on the main emission band which extends into the red and is still increasing at 800 nm (2.0 × intensity at 665 nm, see Figure 9 in the supplementary material).

The luminescence of **4** in 20% aqueous THF solution is dependent upon pH: in acid, λ_{max} 695 nm (relative intensity 1.0); in alkali, λ_{max} 643 nm (relative intensity 2.5) (see Figure 10 in supplementary material). Both the emission maximum and intensity of the related compound $\{Ru^{II}[bpy(C_{19}H_{39})_2][bpy(COOC_2H_5)_2]_2\}^{2+}$ are identical with those of **4** in acidic 20% aqueous THF.[23] The maxima of **4** in $CHCl_3$ solution and as a monolayer film on hydrophilic quartz (alkaline cleaned) transferred from 10^{-3} M $NaClO_4$ are 677 and 671 nm, respectively (Figure 10).

The effect of the counterion is specific to those cases where the positively charged ruthenium complexes **1** and **2** are constrained at the air–water and air–glass interfaces. While the mechanism by which this effect operates is not known, we can eliminate several possibilities. There is no evidence of concentration quenching as chromophores of **1** are brought closer together in monolayers on the chloride subphase even though there is overlap between the absorption and emission spectra.[8] Photochemical reactions involving the excited state of **1** and **2** with counterion could also lead to a reduction in luminescence yield. The oxidation of chloride to atomic chlorine would appear to be eliminated by observing the same luminescence intensity when chloride is replaced by the more easily oxidized bromide. While the presence of iodide anion almost completely quenches the luminescence of **2**, this observation is clouded by the possibility of an alternative reaction with molecular iodine which may have been present in the freshly prepared but air-saturated aqueous subphase. The effect of fluoride is reproducible and was observed by using highly purified NaF. Photoaquation and photoanation have been reported for $Ru^{II}(bpy)_3^{2+}$ in fluid aqueous solution;[24,25] at the 0.1 M level and 343 K, $HClO_4$ causes ca. twofold reduction in photochemical quantum yield from that observed in HCl ($\Phi = 2.93 \times 10^{-4}$)[24]. While irradiated monolayers of **1** in contact with aqueous solutions do slowly degrade ($\Phi \approx 5 \times 10^{-6}$) to unknown products, the presence (10^{-3} M) or absence of either ClO_4^- or Cl^- in the photolyte provides no observable difference by optical spectroscopy or high-pressure LC.

In the absence of irreversible photochemical reaction (and infrared luminescence), radiationless transitions are the main processes which could cause the total emission yield to be less than unity. While the affected electronic transition is different from the $Ru^{II}(bpy)_3^{2+}$ system, perchlorate is known to increase the lifetime and decrease the ligand substitution by H_2O of the ^2E state of $Cr^{III}(bpy)_3^{3+}$ in aqueous solution.[26] The anion is thought to occupy interligand pockets both excluding the H_2O molecule needed in the photoaquation reaction and making the complex more rigid thereby decreasing the rate of radiationless decay. By analogy, the greater rigidity observed for monolayers of **1** and **2** spread on perchlorate- rather than chloride-containing subphases could conceivably account for the emission differences reported here. However, measurements of the absolute luminescence quantum yield in the monolayer state as well as additional information concerning the effect of environment on the photophysics and photochemistry of ruthenium tris(bipyridyl) complexes will be required in order to provide an unambiguous mechanism. It is expected that the control over surface charge afforded by the nonhydrolyzable surfactant complexes described in this report will find use in such studies.

Acknowledgment. The authors wish to thank M. Calvin, G. Porter, and M. Wrighton for helpful discussions leading to the preparation of this report, J. Girard and R. Wentorf for use of their high-pressure LC facilities, and W. Ligon for obtaining the FDMS of the ruthenium bipyridyl complexes. This work was partially supported by the Division of Basic Energy Sciences, U.S. Department of Energy (Grant EG-77-C-02-4395).

Registry No. 1, 59520-37-5; **2a**, 70281-15-1; **2b**, 70281-16-2; **3**, 70281-17-3; **4**, 70288-42-5; **5**, 70281-19-5; **6**, 20506-36-9; **7**, 70281-20-8; **8**, 70268-36-9; **9**, 70268-37-0; **10**, 70281-21-9; *n*-octadecyl chloride, 3386-33-2; $Ru(bpy)_2Cl_2$, 19542-80-4; 4-methylpyridine, 108-89-4.

Supplementary Material Available: The Π–*A* curves for monolayers of **3** and **10** on H_2O (Figure 3), the corrected emission spectra of **3** as a monolayer and in $CHCl_3$ solution and of **6** in H_2O solution (Figure 9), and the corrected emission spectra of **4** in $CHCl_3$ and acidic and basic 20% aqueous THF solution and as a monolayer (Figure 10) (3 pages). Ordering information is given on any current masthead page.

References and Notes

(1) Extensive reference lists are given, for example, by the following: (a) J. N. Demas and J. W. Addington, *J. Am. Chem. Soc.*, **98**, 5800 (1976); (b) D. Meisel, M. S. Matheson, W. A. Mulac, and J. Rabani, *J. Phys. Chem.*, **81**, 1449 (1977).
(2) H. Kuhn, *Chem. Phys. Lipids*, **8**, 401 (1972).
(3) S. J. Valenty in "The Current State of Knowledge of Photochemical Formation of Fuel", N. N. Lichtin, Ed., Boston University, Boston, 1974, p 99.
(4) M. Calvin, *Science*, **184**, 375 (1974).
(5) D. S. Berns, *Photochem. Photobiol.*, **24**, 117 (1976).
(6) S. J. Valenty, *Macromolecules*, **11**, 1221 (1978).
(7) G. Sprintschnik, H. W. Sprintschnik, P. P. Kirsch, and D. G. Whitten, *J. Am. Chem. Soc.*, **99**, 4947 (1977).
(8) G. L. Gaines, Jr., P. E. Behnken, and S. J. Valenty, *J. Am. Chem. Soc.*, **100**, 6549 (1978).
(9) K. P. Seefeld, D. Möbius, and H. Kuhn, *Helv. Chim. Acta*, **60**, 2608 (1977).
(10) L. J. Yellowlees, R. G. Dickinson, C. S. Halliday, J. S. Bonham, and L. E. Lyons, *Aust. J. Chem.*, **31**, 431 (1978).
(11) A. Harriman, *J. Chem. Soc., Chem. Commun.*, 777 (1977).
(12) S. J. Valenty, *J. Am. Chem. Soc.*, **101**, 1 (1979).
(13) J. N. Demas, T. F. Turner, and G. A. Crosby, *Inorg. Chem.* **8**, 674 (1969).
(14) S. J. Valenty and P. E. Behnken, *Anal. Chem.*, **50**, 834 (1978).
(15) G. M. Badger and W. H. F. Sasse, *J. Chem. Soc.*, 616 (1956).
(16) G. L. Gaines, Jr., "Insoluble Monolayers at Liquid-Gas Interfaces", Interscience, New York, 1966, p 212.
(17) See ref 16, p 230.
(18) A. Harriman, private communication.
(19) J. N. Braddock and T. J. Meyer, *Inorg. Chem.*, **12**, 723 (1973).
(20) T. R. Weaver, T. J. Meyer, S. A. Adeyemi, G. M. Brown, R. P. Eckberg, W. E. Hatfield, E. C. Johnson, R. W. Murray, and D. Untereker, *J. Am. Chem. Soc.*, **97**, 3039 (1975).
(21) D. M. Klassen and G. A. Crosby, *J. Chem. Phys.*, **48**, 1853 (1968).
(22) J. N. Demas, J. W. Addington, S. H. Peterson, and E. W. Harris, *J. Phys. Chem.*, **81**, 1039 (1977).
(23) P. E. Behnken, unpublished data.
(24) J. Van Houten and R. J. Watts, *Inorg. Chem.*, **17**, 3381 (1978).
(25) P. E. Hoggard and G. B. Porter, *J. Am. Chem. Soc.*, **100**, 1457 (1978).
(26) M. S. Henry, *J. Am. Chem. Soc.*, **99**, 6138 (1977).